Extended Abstracts of the 2018 International Conference on Solid State Devices and Materials, Tokyo, 2018, pp923-924

Gate-Tuning of Synaptic Functions Based on The Oxygen Vacancy Distribution Control in Four-Terminal TiO_{2-x} Memristive Devices

Zenya Nagata, Takuma Shimizu, Tsuyoshi Isaka, Tetsuya Tohei and Akira Sakai

Graduate School of Engineering Science, Osaka University
1-3, Machikaneyama-cho, Toyonaka-shi
Osaka 560-8531, Japan
Phone: +81-6-6850-6300 E-mail: sakai@ee.es.osaka-u.ac.jp

Abstract

By precise control of oxygen vacancy distribution using various voltage application protocol in four-terminal devices, we have achieved to control the learning ability of synaptic connection, which is a huge step forward towards implementation of high order biological synaptic functions.

1. Introduction

Lots of efforts have been made to achieve hardware implementation of biological synaptic functions in neuromorphic computing. A memristive device is one of promising candidates as an electrical element mimicking the role of synapses in the neural network circuit and a crucial building block for the neuromorphic computer [1,2]. However, it is still challenging to develop the artificial synapse with a hetero-synaptic nature, *i.e.*, modulatable plasticity induced by multiple connections of synapses.

In this study, we fabricate the synaptic devices based on a four-terminals rutile TiO_{2-x} single crystal memristor and demonstrate tunable plasticity by gating operation. In our device, the oxygen vacancy distribution in TiO_{2-x} play a key role in realizing the plasticity of resistance states. Two pairs of electrodes arranged diagonally have different functions: one pair is for read/write operation and the other is for gating operation, which enables precise control of oxygen vacancy distribution. By tuning the gate voltage, we have achieved to modulate the resistance, *i.e.*, potentiation/depletion rate per pulse, and opened the way to control the learning efficiency in neuromorphic devices.

2. Experimental

Fabrication

Reduction of a rutile TiO_2 (001) single crystal substrate was conducted with thermal annealing at 700°C for 6 h under a vacuum of 5×10^{-6} Pa. Planar devices with four terminal electrodes were fabricated on the reduced TiO_{2-x} by depositing square-shaped Pt films through the metal mask. The four electrode terminals were respectively labeled as T1 to T4 as shown in Fig. 1, and T2 and T4 were set to act as the terminals to modulate the oxygen vacancy distribution in the region between T1 and T3.

Potentiation/Depression measurement protocol

First, we applied constant amplitude voltage V_c for a certain period t_c to T2 and T4 while T1 and T3 were grounded. Then, for depression, write voltage pulses V_w with t s width were applied to T1 simultaneously with gate voltage pulses V_g to T2 and T4 while T3 was grounded. For potentiation, the polarity of V_w was changed while T3 was grounded. Device state was checked to measure the resistance between T1 and T3 with a 100 mV amplitude and 100 ms long read voltage pulse application after each write and gate pulse application until it reached the desired high resistance state (HRS) or low resistance state (LRS). Once the device state overshot the HRS or LRS, the write pulse sequence with opposite polarity was employed for potentiation or depletion, respectively.

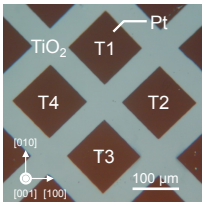

Fig. 1 Optical microscope image of the four terminal device.

Analysis of Ti valence states in RS regions

To clarify the resistance change mechanism, we have also analyzed crystal structures and valence electron states of the TiO_{2-x} electrically active regions in the device using transmission electron microscopy (TEM) and scanning TEM (STEM) in conjunction with electron energy loss spectroscopy (EELS).

3. Results and discussion

Oxygen vacancy distribution and resistance switching

The local concentration of oxygen vacancies is well reflected in the color of the TiO_{2-x} crystal: a region with a higher (lower) concentration of oxygen vacancies is colored (colorless). Furthermore, depending on the morphology of the colored region, the device can be configured to be in HRS or LRS which correspond to the colorless or colored regions formed in the device, respectively. Figures 2(a) and 2(b) show optical microscope images of the device subjected to application of V_c=+6 V and −6 V for t_c=20 s, respectively, and the corresponding resistance values of the device are shown in Fig. 2(c). The observed colored region bridging between T1 and T3 (Fig. 2(a)) well reflects the measured lower resistance between T1 and T3 whereas those bridging between T2 and T4 (Fig. 2(b)) corresponds to the higher resistance. Thus, we can obtain information on the oxygen vacancy distribution, which affects the electrical properties of the memristive device, from a microscopic point of view.

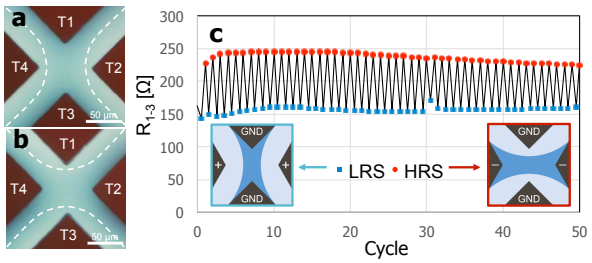

Fig. 2 (a), (b) Optical microscope images of electrically active zone in the device. (c) Measured resistance switching. Blue dots indicate LRS (a), and red dots indicate HRS (b).

TEM and STEM-EELS analysis of device active regions

Figures 3(a) to 3(c) show a TEM image, electron diffraction (ED) pattern, and EELS spectra taken form the LRS region in the device. While no significant change from the rutile structure is observed, the analysis of EELS spectrum (decrease in peak splitting width of Ti-L_3 edge) indicates that LRS has reduced Ti valence states due to the oxygen vacancy redistribution. This valence state change without crystal structure change should be the origin of the reversible resistance switching behavior shown in Fig. 2(c) in the present memristive device.

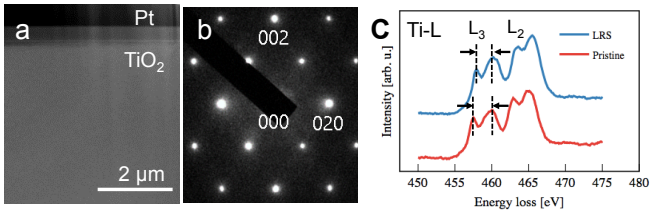

Fig. 3 TEM image (a) and ED pattern (b) observed at the LRS region. (c) Ti-$L_{2,3}$ EELS spectra of LRS region (blue line) and pristine sample (red line).

Multilevel resistance by consecutive voltage sweeps

We have demonstrated that multilevel resistance between T1 and T3 can be achieved by changing the applied voltage sweep rate. As shown in Fig. 4(a), the incremental resistance tended to be saturated after applying the sweep voltage V_1=+6 V to T1 several times at a certain sweep rate.

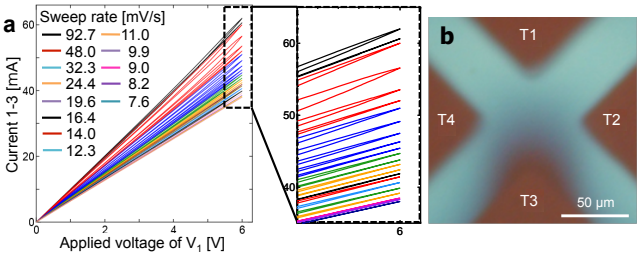

Fig. 4 (a) Current-voltage characteristics obtained by consecutive voltage sweeps. Each colored lines show hysteresis curves by varying the voltage sweep rate of V_1 shown in the inset. (b) Optical microscope image of the device after the consecutive sweeps.

However, the reduction of the sweep rate leads to further increase of resistance. This incremental resistance modulation can be explained by the colorless region around T1 indicating oxygen vacancy repulsion from T1 as shown in Fig. 4(b). Thus, by selecting appropriate voltage sweep rate, we can achieve high precision tuning of resistance, or plasticity of synapse.

Gate control of synaptic plasticity

We have explored the possibility of controlling potentiation/depression sensitivity (or synaptic plasticity) by gate voltage application according to the designated protocol. As shown in Fig. 5, the number of pulses required to reach the desired resistance can be modulated by the gate voltage: higher the gate voltage is, smaller the number of required pulses is. This demonstrates a pair of electrodes for gating can mimic the function of neuromodulator which can regulate the plasticity of synapse in its vicinity, providing a hetero-synaptic nature for highly complicated behaviors of living creatures.

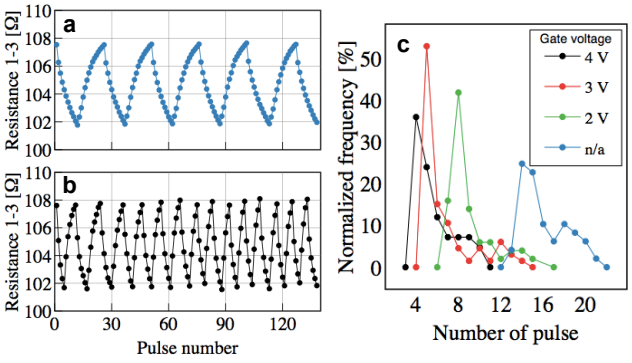

Fig. 5 Resistance switching of the device (a) without and (b) with the gate voltage V_g = 4 V. (c) Gate voltage dependency of the number of pulse required to reach the desired HRS. The parameter was set to V_c = 6 V, t_c = 50 s, t = 10 s and V_w = ±4 V.

4. Conclusions

We have explored the possibility of variable synaptic behavior based on precise control of oxygen vacancy distribution in single crystal TiO_{2-x} four-terminal memristive devices. Our results demonstrate that by tuning the voltage application protocol, that is, changing voltage sweep rates or gate voltages application, potentiation/depression behavior (*i.e.*, synapse plasticity) can be markedly modulated to achieve the function of neuromodulator in living synapses.

Acknowledgements

This work was supported by a KAKENHI Grant-in-Aid (Nos. JP17H03236, and JP17K18881) from the Japan Society for the Promotion of Science (JSPS) and a grant from the Murata Science Foundation.

References

[1] D. B. Strukov et al., Nature 453, 80 (2008).
[2] M. Prezioso et al., Nature 521, 61 (2015).